Prismatic spreading-constriction expression for the improvement of impedance spectroscopy models and a more accurate determination of the internal thermal contact resistances of thermoelectric modules

Mutabe Aljaghtham[1], Ge Song[2], Jorge García-Cañadas[3], and Braulio Beltrán-Pitarch[4,*]

[1]*Department of Mechanical Engineering, Prince Sattam Bin Abdulaziz University, Al-Kharj 16278, Saudi Arabia*

[2]*College of Civil Engineering, Hunan University, Changsha, 4100182 Hunan, China*

[3]*Department of Industrial Systems Engineering and Design, Universitat Jaume I, Campus del Riu Sec, 12006 Castelló de la Plana, Spain*

[4]*DTU Energy – Department of Energy Conversion and Storage, Technical University of Denmark, Fysikvej 310, DK-2800 Kgs Lyngby, Denmark*

[*]*e-mail: brapit@dtu.dk*

SPREADING-CONSTRICTION DERIVATIONS

This supporting information shows the derivations needed to obtain the impedance response due to the spreading-constriction in prismatic layers. The two-layer structure can be seen in Figure S1, and it consists of a metallic strip (with area $x_1 \times y_1$) in contact with a ceramic (with length L_C) of larger cross-sectional area ($x_2 \times y_2$). The metallic strip, which has a negligible thickness, is considered to apply a uniform heat flux φ_0 into the ceramic.

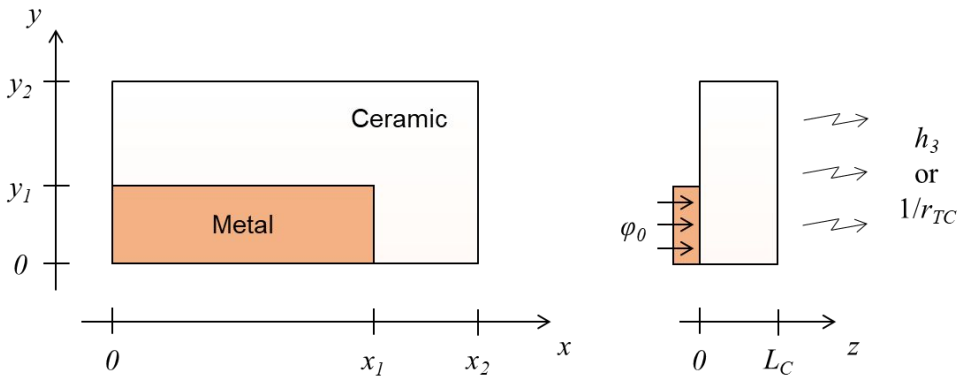

Figure S1. Schematic drawing of the theoretical model used to calculate the impedance due to the spreading-constriction. Not to scale.

The first step to calculate the spreading-constriction impedance is to obtain the temperature, T, distribution inside the ceramic layer. This is solved starting from the general heat equation,

$$\frac{\partial T(x,y,z)}{\partial t} = \alpha_C \nabla^2 T(x,y,z), \tag{S1}$$

where α_C is the thermal diffusivity of the ceramic material, and the coordinates (x, y, z) define all points inside the ceramic material. This equation in the frequency domain becomes,

$$j\omega\theta(x,y,z) = \alpha_C \nabla^2 \theta(x,y,z), \tag{S2}$$

where, $j=(-1)^{0.5}$ is the imaginary number, ω the angular frequency ($\omega=2\pi f$, where f is the frequency), and θ is the temperature rise/decrease with respect to the ambient temperature in the frequency domain.

The separation of variables allow us to define the temperature as three different functions that only depend on one coordinate,

$$\theta(x,y,z) = U(x)V(y)W(z). \tag{S3}$$

Then, we can rewrite eq. (S2) into,

$$\frac{j\omega}{\alpha_C} = \frac{U''}{U} + \frac{V''}{V} + \frac{W''}{W}, \tag{S4}$$

and define three constants (α, β, γ) so that,

$$\frac{U''}{U} = -\alpha^2, \tag{S5}$$

$$\frac{U''}{U} = -\beta^2, \tag{S6}$$

$$\frac{W''}{W} = \gamma^2, \tag{S7}$$

$$\frac{j\omega}{\alpha_C} = -\alpha^2 - \beta^2 + \gamma^2. \tag{S8}$$

The solutions of eq. (S5), eq. (S6), and eq. (S7) can be written as,

$$U(x) = C_1 cos\,(\alpha x) + C_2 sin\,(\alpha x), \tag{S9}$$

$$V(y) = C_3 cos\,(\beta y) + C_4 sin\,(\beta y), \tag{S10}$$

$$W(z) = C_5 cosh\,(\gamma z) + C_6 sinh\,(\gamma z), \tag{S11}$$

where C_1, C_2, C_3, C_4, C_5, and C_6 are constants.

On the other hand, the boundary conditions of our system are (see Figure S1),

$$\left(\frac{\partial\theta}{\partial x}\right)_{x=0} = 0, \tag{S12}$$

$$\left(\frac{\partial\theta}{\partial x}\right)_{x=x_2} = 0, \tag{S13}$$

$$\left(\frac{\partial\theta}{\partial y}\right)_{y=0} = 0, \tag{S14}$$

$$\left(\frac{\partial\theta}{\partial y}\right)_{y=y_2} = 0, \tag{S15}$$

$$\left(\frac{\partial\theta}{\partial z}\right)_{z=0} = -\frac{\varphi_0}{\lambda_C}, \text{ if } 0 < x \le x_1 \text{ and } 0 < y \le y_1, \tag{S16}$$

$$\left(\frac{\partial\theta}{\partial z}\right)_{z=0} = 0, \text{ otherwise}, \tag{S17}$$

$$\left(\frac{\partial\theta}{\partial z}\right)_{z=L_C} = -\frac{h_3\theta_{z=L_C}}{\lambda_C}, \tag{S18}$$

where h_3 is the convection coefficient at $z=L_C$ (in contacted TE devices, it can be substituted by a thermal contact resistivity $r_{TC}=1/h_3$), and λ_C is the thermal conductivity of the ceramic material.

From eq. (S12) and eq. (S14) it is directly obtained that $C_2=0$ and $C_4=0$, respectively. Then, using eq. (S13) and eq. (S15) we find all the values of $\alpha_n=n\pi/x_2$ and $\beta_m=m\pi/y_2$ that are solutions to this problem (n and m can be any non-negative integers). In this way, to satisfy eq. (S8), we obtain,

$$\gamma_{n,m} = \sqrt{\left(\frac{n\pi}{x_2}\right)^2 + \left(\frac{m\pi}{y_2}\right)^2 + \frac{j\omega}{\alpha_C}}, \tag{S19}$$

At this point, the temperature expression takes the form,

$$\theta(x,y,z) = \sum_{n,m=0}^{\infty} C_{1,n}cos\,(\alpha_n x)C_{3,m}cos\,(\beta_m y)[C_{5,n,m}cosh\,(\gamma_{n,m}z) + C_{6,n,m}sinh\,(\gamma_{n,m}z)], \tag{S20}$$

and its derivative with respect to z,

$$\frac{\partial\theta}{\partial z} = \sum_{n,m=0}^{\infty} C_{1,n}cos\,(\alpha_n x)C_{3,m}cos\,(\beta_m y)\gamma_{n,m}[C_{5,n,m}sinh\,(\gamma_{n,m}z) + C_{6,n,m}cosh\,(\gamma_{n,m}z)]. \tag{S21}$$

Introducing eq. (S20) and eq. (S21) into eq. (S18) and evaluating at $z=L_C$, the ratio between $C_{6,n,m}$ and $C_{5,n,m}$ is obtained,

$$R_{n,m} = -\frac{C_{6,n,m}}{C_{5,n,m}} = \left[\frac{\gamma_{n,m}sinh\,(\gamma_{n,m}L_C) + \frac{h_3}{\lambda_C}cosh\,(\gamma_{n,m}L_C)}{\gamma_{n,m}cosh\,(\gamma_{n,m}L_C) + \frac{h_3}{\lambda_C}sinh\,(\gamma_{n,m}L_C)}\right]. \tag{S22}$$

The temperature can then be written as,

$$\theta(x,y,z) = \sum_{n=1}^{\infty} C_n cos\,(\alpha_n x)[cosh\,(\gamma_n z) - R_n sinh\,(\gamma_n z)] + \sum_{m=1}^{\infty} C_m cos\,(\beta_m y)[cosh\,(\gamma_m z) - R_m sinh$$
$$+ \sum_{n,m=1}^{\infty} C_{n,m} cos\,(\alpha_n x)cos\,(\beta_m y)[cosh\,(\gamma_{n,m}z) - R_{n,m}sinh\,(\gamma_{n,m}z)]. \tag{S23}$$

where it is also necessary to define,

$$\gamma_n = \sqrt{\left(\frac{n\pi}{x_2}\right)^2 + \frac{j\omega}{\alpha_C}}, \tag{S24}$$

$$\gamma_m = \sqrt{\left(\frac{m\pi}{y_2}\right)^2 + \frac{j\omega}{\alpha_C}}, \tag{S25}$$

$$R_n = -\frac{C_{6,n}}{C_{5,n}} = \left[\frac{\gamma_n sinh\,(\gamma_n L_C) + \frac{h_3}{\lambda_C} cosh\,(\gamma_n L_C)}{\gamma_n cosh\,(\gamma_n L_C) + \frac{h_3}{\lambda_C} sinh\,(\gamma_n L_C)}\right], \tag{S26}$$

$$R_m = -\frac{C_{6,m}}{C_{5,m}} = \left[\frac{\gamma_m sinh\,(\gamma_m L_C) + \frac{h_3}{\lambda_C} cosh\,(\gamma_m L_C)}{\gamma_m cosh\,(\gamma_m L_C) + \frac{h_3}{\lambda_C} sinh\,(\gamma_m L_C)}\right]. \tag{S27}$$

Deriving, and evaluating at z=0,

$$\left.\frac{\partial\theta(x,y,z)}{\partial z}\right|_{z=0} = -\sum_{n=1}^{\infty} C_n cos\,(\alpha_n x)\gamma_n R_n - \sum_{m=1}^{\infty} C_m cos\,(\beta_m y)\gamma_m R_m - \sum_{n,m=1}^{\infty} C_{n,m} cos\,(\alpha_n x) cos\,(\beta_m y \tag{S28}$$

Introducing eq. (S28) into eq. (S16) and eq. (S17), multiplying by $\cos(n\pi x/x_2)$, integrating from 0 to x_2, multiplying again by $\cos(m\pi y/y_2)$, and integrating from 0 to y_2, after some algebraic steps we obtain,

$$C_n = \frac{2\varphi_0 sin\,(\alpha_n x_1) y_1}{\lambda_C n\pi\gamma_n R_n y_2}, \tag{S29}$$

$$C_m = \frac{2\varphi_0 sin\,(\beta_m y_1) x_1}{\lambda_C m\pi\gamma_m R_m x_2}, \tag{S30}$$

$$C_{n,m} = \frac{4\varphi_0 sin\,(\alpha_n x_1) sin\,(\beta_m y_1)}{\lambda_C nm\pi^2\gamma_{n,m} R_{n,m}}. \tag{S31}$$

So that the temperature at z=0, and the spreading-constriction impedance are given by,

$$\theta(x,y,0) = \sum_{n=1}^{\infty} C_n cos\,(\alpha_n x) + \sum_{m=1}^{\infty} C_m cos\,(\beta_m y) + \sum_{n,m=1}^{\infty} C_{n,m} cos\,(\alpha_n x) cos\,(\beta_m y), \tag{S32}$$

$$z_{s/c} = \frac{\overline{\theta}(x,y,0)}{\varphi_0} = \frac{\int_0^{y_1}\int_0^{x_1}\theta(x,y,0)\,\partial x\partial y}{\varphi_0 x_1 y_1}, \tag{S33}$$

where the constants C_n, C_m, and $C_{n,m}$ are defined by eq. (S29), eq. (S30), and eq. (S31), respectively.

Hence, the spreading-constriction impedance is,

$$z_{s/c} = \frac{2x_2y_1}{\lambda_C\pi^2x_1y_2}\sum_{n=1}^{\infty}\frac{sin^2(\alpha_n x_1)}{n^2\gamma_n}\left[\frac{\gamma_n\lambda_C + h_3 tanh(\gamma_n L_C)}{\gamma_n\lambda_C tanh(\gamma_n L_C) + h_3}\right] + \frac{2y_2x_1}{\lambda_C\pi^2y_1x_2}\sum_{m=1}^{\infty}\frac{sin^2(\beta_m y_1)}{m^2\gamma_m}\left[\frac{\gamma_m\lambda_C + h_3 tanh}{\gamma_m\lambda_C tanh(\gamma_m l}\right. \quad \text{(S34)}$$
$$+ \frac{4x_2y_2}{\lambda_C\pi^4x_1y_1}\sum_{n,m=1}^{\infty}\frac{sin^2(\alpha_n x_1)sin^2(\beta_m y_1)}{n^2m^2\gamma_{n,m}}\left[\frac{\gamma_{n,m}\lambda_C + h_3 tanh(\gamma_{n,m}L_C)}{\gamma_{n,m}\lambda_C tanh(\gamma_{n,m}L_C) + h_3}\right].$$

And in the limit where $\omega \to 0$, the spreading-constriction resistance matches the expression obtained by Muzychka et al.,[30] which adapted to our nomenclature, can be defined as,

$$r_{s/c} = \frac{2{x_2}^2y_1}{\lambda_C\pi^3x_1y_2}\sum_{n=1}^{\infty}\frac{sin^2(\alpha_n x_1)}{n^3}\left[\frac{\alpha_n\lambda_C + h_3 tanh(\alpha_n L_C)}{\alpha_n\lambda_C tanh(\alpha_n L_C) + h_3}\right] + \frac{2{y_2}^2x_1}{\lambda_C\pi^3y_1x_2}\sum_{m=1}^{\infty}\frac{sin^2(\beta_m y_1)}{m^3}\left[\frac{\beta_m\lambda_C}{\beta_m\lambda_C t}\right. \quad \text{(S35)}$$
$$+ \frac{4x_2y_2}{\lambda_C\pi^4x_1y_1}\sum_{n,m=1}^{\infty}\frac{sin^2(\alpha_n x_1)sin^2(\beta_m y_1)}{n^2m^2\delta_{n,m}}\left[\frac{\delta_{n,m}\lambda_C + h_3 tanh(\delta_{n,m}L_C)}{\delta_{n,m}\lambda_C tanh(\delta_{n,m}L_C) + h_3}\right],$$

where $\delta_{n,m}=(\alpha_n{}^2+\beta_m{}^2)^{1/2}$.

NUMERICAL VALIDATION

To quantify the deviations in the determination of the internal thermal contact resistances, a COMSOL simulation was performed, which will be considered as an experimental measurement. The FEM simulation was performed using the *electric currents*, the *heat transfer* and the *thermoelectric* packages of COMSOL. Initial steady conditions of temperature (300 K) and potential (0 V) were considered, and adiabatic boundary conditions in all surfaces were used. A sinusoidal current of 10 mA was injected at one side of the TE leg and extracted at the other, while the voltage at the same locations was recorded. In addition, convergence tests assured a properly meshed geometry and short enough time steps taken by the time-dependent solver. The simulated voltage waveforms of each frequency (36 logarithmically distributed points from 10 mHz to 100 kHz) were introduced in a numerical lock-in amplifier implemented in MATLAB to extract the amplitudes and phases.

Typical values of commercial thermoelectric devices at T=300 K were used (N=127, S=190 μVK^{-1}, ρ_{TE}=1 mΩcm, λ_{TE}=1.5 Wm^{-1}K^{-1}, α_{TE}=0.37 mm^{2}s^{-1}, L=1.2 mm, λ_M=400 Wm^{-1}K^{-1}, α_M=110 mm^{2}s^{-1}, L_M=0.3 mm, λ_C=35 Wm^{-1}K^{-1}, α_C=10 mm^{2}s^{-1}, L_C=0.75 mm, A=1.69 mm^2, η=0.27, and η_M=0.68). A thermal contact resistivity between the TE legs and the metallic strips, r_{TCI}=1.26×10^{-5} m^{2}KW^{-1}, and an inductance, L_p=4×10^{-7} H, were also added. Figure S2 shows the simulated impedance spectra (dots), the fitting using the cylindrical approximation (red line, Fit-C in the legend), and the fitting with the new spreading-constriction impedance (in blue, Fit-P in the legend).

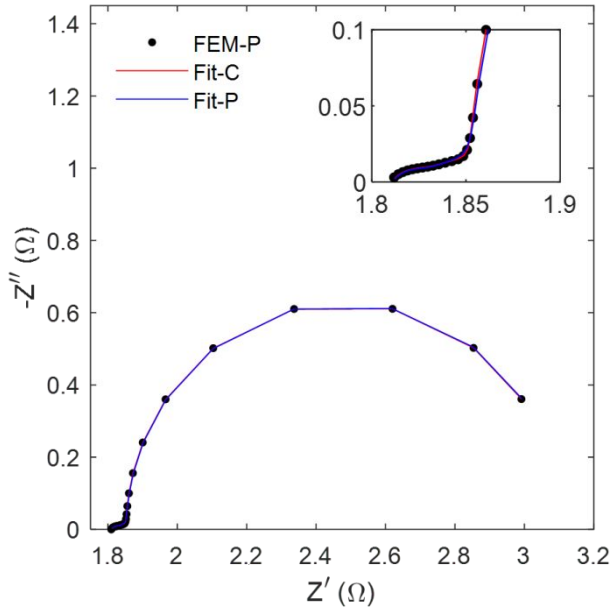

Figure S2. FEM impedance simulations (dots) and their fittings (lines). C and P in the legend indicates cylindrical and prismatic geometries, respectively.

From the first fitting in Figure S2 (red line), an estimation of the error when fitting a commercial device (prismatic structure) with the cylindrical approximation can be calculated. Then, from the second fitting in Figure S2 (blue line), the improvement due to the development of the analytical expression for prismatic structures can be evaluated. The fitted values and their associated relative errors can be found in Table S1. Low fitting errors in all

cases were obtained (mostly below 1%). In addition, the deviations of the fitted parameters from the COMSOL simulations can be seen in Table S2. The ohmic resistance, R_{Ω}, and the thermal conductivities (λ_{TE}, and λ_{C}), showed deviations lower than 0.4% with respect to the expected values (see Table S2). However, the thermal contact resistivity between the TE legs and the metallic strips (r_{TCI}) was overestimated 4.2% when the cylindrical approximation was used. This thermal contact resistance was only overestimated by 0.3% when the new spreading-constriction impedance (developed in this study) was used.

Table S1. Fitting parameters with their associated relative errors (in brackets). The fittings using the cylindrical model were performed with the MATLAB code provided in the Supplementary Information of ref..[25] The fitting with the prismatic model was performed with the MATLAB code provided in the Supplementary Information of this article.

Model	R_{Ω} (Ω)	r_{TCI} (m^2KW^{-1})	λ_{TE} ($Wm^{-1}K^{-1}$)	λ_{C} ($Wm^{-1}K^{-1}$)
Prismatic data fitted with cylindrical model	1.8033 (0.00294%)	1.3128×10^{-5} (0.253%)	1.4994 (0.0508%)	34.997 (0.0621%)
Prismatic data fitted with prismatic model	1.8036 (0.0125%)	1.2637×10^{-5} (1.10%)	1.4976 (0.197%)	35.126 (0.238%)

Table S2. Values introduced in the COMSOL simulations (expected values), and deviations of the fitted parameters (shown in Table S1).

	R_{Ω} (Ω)	r_{TCI} (m^2KW^{-1})	λ_{TE} ($Wm^{-1}K^{-1}$)	λ_{C} ($Wm^{-1}K^{-1}$)
Expected value	1.8036	1.26×10^{-5}	1.5	35
Prismatic data fitted with cylindrical model	-0.02%	4.19%	-0.04%	-0.01%
Prismatic data fitted with prismatic model (new)	0.00%	0.29%	-0.16%	0.36%